

MULTIFRACTAL PROPERTIES OF REMOTELY SENSED RAINFALL FIELDS

L. FERRARIS^a, U. PARODI^a AND R. DEIDDA^b

^a*Centro di ricerca in monitoraggio ambientale, University of Genoa, Vi
cadorna 7, 17100 Savona, Italy – e-mail: lf@cima.unige.it*

^b*Centro di Ricerca, Sviluppo e Studi Superiori in Sardegna, C.P. 94, Cagliari
Italy - e-mail: Roberto.Deidda@crs4.it*

Abstract

The resolution of precipitation fields forecasted by atmospheric models typically ranges from about 10^2 to 10^4 Km² in space and from few hours to few days in time, while the resolution of interest when modelling runoff in complex orography areas is of the order of a square kilometer in space and a few minutes in time. Many studies have investigated the scale properties of precipitation fields; these show the presence of a scale-invariant organization that seems to reflect the physical properties of the processes. Scale invariance helps to develop efficient rainfall downscaling schemes to be used in a coupled atmospheric-hydrologic approach. Multifractal models allow to capture the moments of the observed rainfall signals throughout different scales and are expected to be successfully applied in rainfall disaggregation tools. The temporal persistence of the process suggests the use of models that preserve multifractal properties observed in real rainfall both in time and in space. In the present work are presented:

- i) the case-study of a space-time (3D) multifractal analysis for rainfall fields derived by a terrain based radar (FOSSALON);
- ii) the comparison with results of a similar analysis carried out in space (2D) for different sensor derived rainfall fields (SSM/I).

1 Introduction

One of the most important problems concerning any real time flood prediction is the lack of knowledge of the small-scale statistical properties of the convective rainfall fields.

In many tropical and mid latitude areas, characterized by complex orography drained by small size river catchments, rainfall events producing heavy floods show high convective components. The small size of the river catchments reduces the characteristic response time to heavy rainfall to few hours. Therefore any reliable real time flood prediction tool aimed at early warning to the population has to use rainfall predictions coupled to rainfall-runoff models.

The operational experience has highlighted that a gap exists between the scales solved by meteorological and hydrological models. Hydrologists attempt to fill this gap using statistical disaggregation models, able to simulate rainfall fields at scales smaller than those of the meteorological prediction.

The small number of reliable datasets makes it difficult to acknowledge the capacity of disaggregation models in reproducing “observed” rainfall fields statistics.

The remote observations based on ground radar and meteorological satellite, such as DMSP (Defence Meteorological Satellite Program) and TRMM (Tropical Rainfall Measuring Mission), give an important contribution to the building of these datasets, providing multiscale observations of the convective rainfall fields. Therefore it is important to investigate how radar derived rainfall fields can be used in disaggregation models.

The data provided by a ground based radar and the SSM/I sensors are used here to investigate the multifractal properties [Feder, 1988; Falconer, 1990] of the convective rainfall fields.

The multifractal properties of the rainfall fields obtained from the analysis will be used to find the parameters of a multifractal downscaling model [Deidda, et al., 1999; Deidda 1999a, 1999b].

These analyses represent an important improvement of the real time flood prediction, allowing better evaluations of the response of river basins to extreme rainfall events.

This paper is organized as follows: in section 2 we discuss the space-time multifractal modeling of rainfall fields; Section 3 is devoted to space and space-time multifractal analysis of SSM/I and ground based radar rainfall-fields of the Friuli event of October 1998. In section 4 the conclusions of this work are drawn.

2 Multifractal modeling of rainfall fields

In this section it is shown how to construct synthetic fields of space-time rainfall with prescribed multifractal behaviour using the STRAIN (Space-Time RAINfall) model [Deidda, 1999b]

The model is a generalization of the multidimensional model by Deidda et al. [1999] and so includes generalized scaling and scale covariance by means of

an infinitely divisible log-Poisson distribution [Dubrulle, 1994; She and Leveque, 1994].

The model assumes that rainfall fields are isotropic and statistically homogeneous in space and that self-similarity holds, so that we can rescale the time dimension by the advection velocity U (Taylor hypothesis [Taylor, 38]) to obtain a fully homogeneous and isotropic process in the space-time domain.

A synthetic space-time rainfall intensity field $i(x,y,t)$ with $(x,y) \in [0,L]^2$ and $t \in [0,T]$, where $T=L/U$, is obtained as a wavelet expansion with coefficients extracted by a stochastic cascade:

$$i(x, y, t) = \sum_{j=0}^N \sum_{kx=0}^{2^j-1} \sum_{ky=0}^{2^j-1} \sum_{kt=0}^{2^j-1} \alpha_{j,kx,ky,kt} \psi_{j,kx,ky,kt}(x, y, t) \quad (1)$$

where $\psi_{j,kx,ky,kt}(x,y,t)$ is a wavelet on level j with position kx,ky,kt and $\alpha_{j,kx,ky,kt}$ is the coefficient extracted from the stochastic cascade.

The three-dimensional wavelet $\psi(x,y,t)$ is defined as a product of three one-dimensional basis wavelets $\Psi(z)$, positive definite and integrable for $z \in [0, L]$ and zero elsewhere:

$$\psi_{j,kx,ky,kt}(x, y, t) = 2^{3j} \Psi(2^j x - kxL) \Psi(2^j y - kyL) \Psi(2^j Ut - ktL) \quad (2)$$

The normalisation in modulus of the basis function $\psi(z)$ assures the normalisation of each wavelet $\psi(x,y,t)$, defined by the above equation. The following Gaussian distribution is an example of the basis wavelet used:

$$\Psi(z) = \begin{cases} c \exp[-0.5((z-\mu)/\sigma)^2] & z \in [0, L] \\ 0 & z \notin [0, L] \end{cases} \quad (3)$$

where $m=L/2$, $s=0.15L$ and $c \approx 1/(\sigma\sqrt{2\pi})$ is a normalization constant.

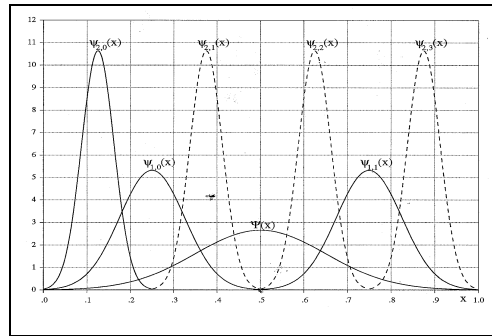


Figure 2.1: Gaussian basis function $\Psi(z)$, defined by equation (3) with $s = 0.15$ and onedimensional wavelets $\psi_{j,k}(x)$ for the first two levels $j=1,2$, obtained by stretching and shifting the same basis function $\Psi(z)$. The integral of each wavelet is normalized to unity.

The random cascade is constructed using a multiplicative process; each *son* $a_{j,kx,ky,kt}$ at the j -th level is obtained by multiplying the corresponding *father* at level $j-1$ by an independent and identically distributed random variable h , called generator:

$$\alpha_{j,kx,ky,kt} = \alpha_{j-1, \frac{kx}{2}, \frac{ky}{2}, \frac{kt}{2}} \eta \quad (4)$$

The structure functions $S_q(1)$ of signals (1) can be defined as:

$$S_q(\lambda) = \left\langle \left[\int_{\xi}^{\xi+\lambda} dx \int_{\eta}^{\eta+\lambda} dy \int_{\sigma}^{\sigma+\lambda/U} dt i(x, y, t) \right]^q \right\rangle \propto \lambda^{\zeta(q)} \quad (5)$$

where $\langle \dots \rangle$ is the spatial average.

After some computations it can be shown that structure functions obey anomalous scaling $S_q(1) \sim 1^{z(q)}$ with multifractal exponents $z(q)$, depending only on the ensemble averages of the moments of the generator η :

$$\zeta(q) = q(3 + \log_2 \bar{\eta}) - \log_2 \bar{\eta}^q \quad (6)$$

The choice of the probability distribution of the random generator h characterises the multifractal behaviour of the synthetic signals. In this work the log-Poisson distribution was used:

$$\eta = e^A \beta^y; \quad P(y = m) = \frac{c^m e^{-c}}{m!} \quad (7)$$

where A and β are constant parameters, while y is a Poisson distributed random variable with average c : $E[y]=c$.

The expected scaling of signals can be finally evaluated:

$$\zeta(q) = 3q + c \frac{q(\beta - 1) - (\beta^q - 1)}{\ln 2} \quad (8)$$

where the multifractal exponent $z(q)$ depends only on the parameters c and β .

Estimates of the model parameters c and b can be obtained by solving the following minimization problem:

$$\min_{c, \beta} \sum_q \left[\frac{\hat{\zeta}(q) - \zeta(q)}{\sigma(q)} \right]^2 \quad (9)$$

where $\hat{\zeta}(q)$ are the sample multifractal exponents, $\zeta(q)$ is the theoretical expectation, $\sigma(q) = q - 1$ is a weight that accounts for the estimation error, i.e. the standard deviation of $\hat{\zeta}(q)$.

3 Multifractal analysis of rainfall fields

The data used for the multifractal analysis in space and space-time come from two different sensors:

- the C-banded polarimetric doppler radar FOSSALON of Grado (GO), sited in the north east of Italy at 45.73 latitude and 13.5 longitude that sweeps a circular area of diameter 245 Km with a resolution of about .125 Km every ten minutes;
- the Special Sensor Microwave/Imager (SSM/I) aboard the Defence Meteorological Satellite Program (DMSP) Block 5D-2 Spacecraft F8 that has a swath width of 1394 Km and an EFOV on earth surface at different frequency bands that go from 70 to 13 Km. The SSM/I sweeps the study area on average every 12 hours.

The rainfall fields from the FOSSALON radar images were estimated by the Weather Radar Operation Center of the “Ente Regionale per lo Sviluppo Agricolo della Regione Friuli”, Italy, while the SSM/I derived rainfall field was estimated by of the Istituto di Fisica dell’Atmosfera, CNR Roma Italy, and has a resolution of about 25 Km.

In space the multifractal analysis was performed on the following data set:

- 41 radar images given at 30 minutes (the rainfall intensity is average on 10 minutes) going from the 19:50 GMT of the 6th of October 1998 to the 15:50 GMT of the 7th of October 1998.
- 2 SSM/I images corresponding to the same hour 5:33 GMT of the 7th of October 1998, on two different spatial domains: one - extracted SSM/I field – has size of about 800 km and is centered on the Trentino region, the second - total SSM/I field – has size of about 1600 km. The rainfall intensity was given about every 5 minutes The radar image of hour 5:28 GMT corresponds to the SSM/I passage.

In space-time the multifractal analysis was performed on the data set of 112 radar images given at 10 minutes intervals going from the 19:49 GMT of the 6th of October 1998 to the 14:18 GMT of the 7th of October 1998.

The event lasted from the 5th to the 8th of October with the highest intensity rainfalls between the 6th and the 7th. The total rainfall measured at Caporetto and Udine has been of about 400 mm in 48 hours. The event caused over-bank flow for the subcatchments of the Latisone (300 Km²) and full bank flow in most of the sub-basins of the area, such as Tagliamento and Piave.

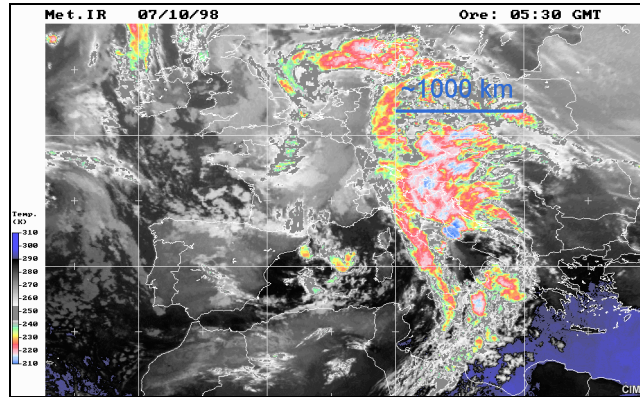


Figure 3.1: Meteosat infrared image. Typical cloud structure observed during the extreme event of October 1998. A wide area, dark blue and red, shows lower cloud top radiance temperatures and therefore high probability of convective activity. The convective area has a spatial domain of about 1000 km.

3.1 SPACE ANALYSIS

Structure functions, in space, were computed on radar and SSM/I rainfall fields: the spatial radar scale ranges from 0.5 km to 128 km, while the SSM/I field scale ranges from 25 km to 800 km. In Figure 3.2 and Figure 3.3 the structure functions for the first six moments of the fields from the two different sensors are plotted in the log-log plane.

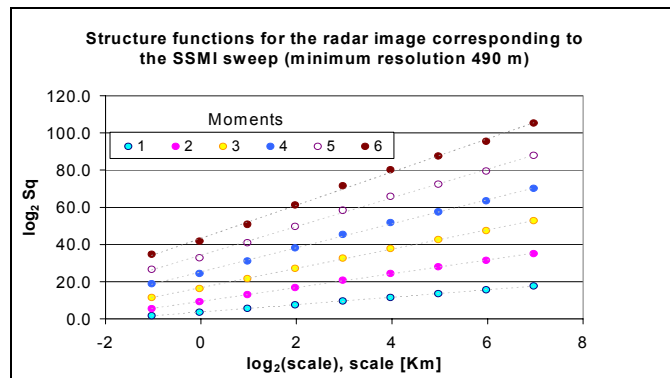


Figure 3.2: the first six space structure functions $S_q(r)$ estimated on 41 radar images at 30 minutes interval from 19:50 GMT - 6th of October 1998 to 15:50 GMT - 7th of October 1998. The rainfall intensity is average on 10 minutes. The space scales range from 0.5 km to 128 km. The scaling of structure functions is highlighted by the log-log least squares regressions.

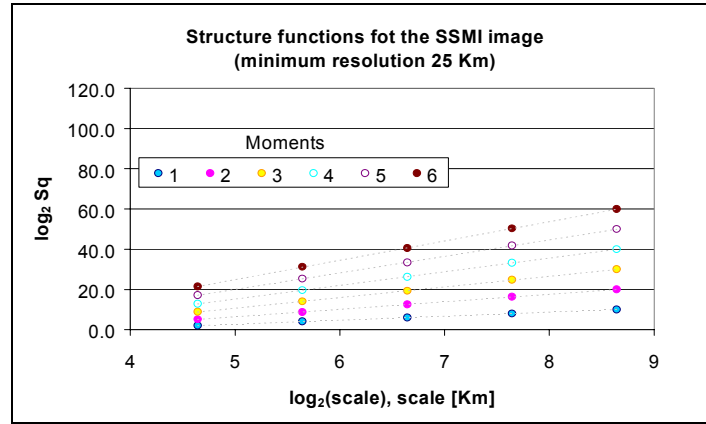


Figure 3.3: the first six structure functions $S_q(r)$ estimated on one SSM/I field – extracted SSM/I image- corresponding hour 5:33 GMT - 7th of October 1998. The space scales range from 25 km to 800 km. The scaling of structure functions is highlighted by the log-log least squares regressions.

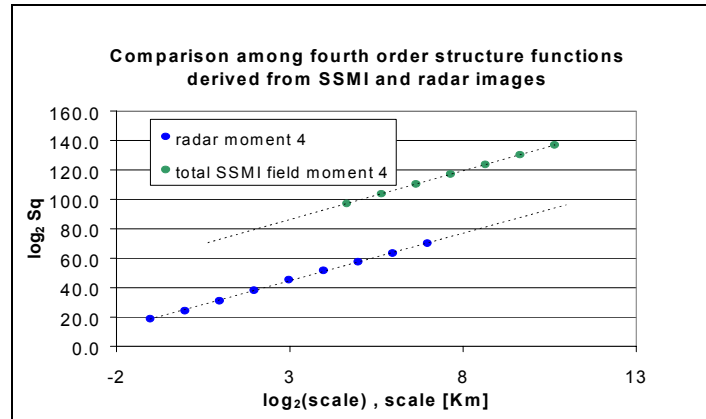


Figure 3.4: comparison between the structure functions $S_q(r)$ of the fourth moment, estimated on 41 radar images and on the total SSM/I field image. The total SSM/I field is contemporary the 21th radar image. The scaling of structure functions is clearly similar: the range of space scale is from 0.5 km to 1600 km.

The slopes of the structure functions, obtained for the radar and SSM/I, are very similar therefore the multifractal exponents $z(q)$ can be considered unique for scale ranging from 0.5 km to 1600 km, as shown by Figure 3.4 where the fourth-order structure functions of radar and SSM/I data are compared.

Multifractal exponents $z(q)$ are estimated by linear regression of structure function $S_q(1)$ versus 1 in the log-log plane for the two different sensors and are presented in Figure 3.5.

In the same figure are plotted also the multifractal exponents of rainfall spatial fields at duration of 15 minutes and 24 hours, based on the radar observations during the GATE 1 campaign (GARP, Global Atmospheric Research Program, Atlantic Tropical Experiment). A more detailed discussion on results of the multifractal analysis of GATE rainfall fields in space can be found in Deidda, 1999a.

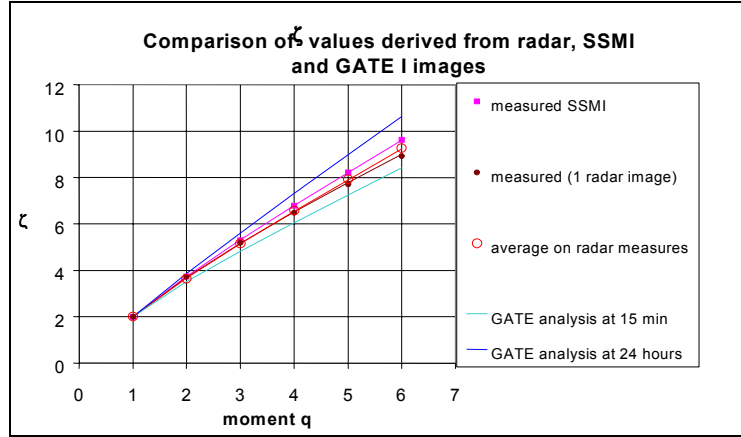


Figure 3.5: results are compared. Exponents $z(q)$ evaluated from the SSM/I field image (squares), the contemporary radar image (black dots) and 41 radar images (wild dots) show relevant agreement among them. Results are also compared with the multifractal exponents estimated from GATE1 datasets for two durations: 15-minute and 24-hour.

Sample multifractal exponents (from $q=2$ to 6) are then used to estimate the two log-Poisson parameters c and b of the model by solving the minimization problem (9). Results for the two sensors are similar and have shown that the b parameter can be considered constant for all the analyzed fields and equal to its mean values $b=0.5$ independently of the amount of rainfall.

The minimization problem (9) was solved again, but keeping constant the b parameter, fixed at its mean value 0.5. The new estimate of the c parameter for both radar and SSM/I data are plotted versus the spatial average of rainfall intensity in Figure 3.6, where a decreasing trend with increasing mean rainfall intensity is apparent.

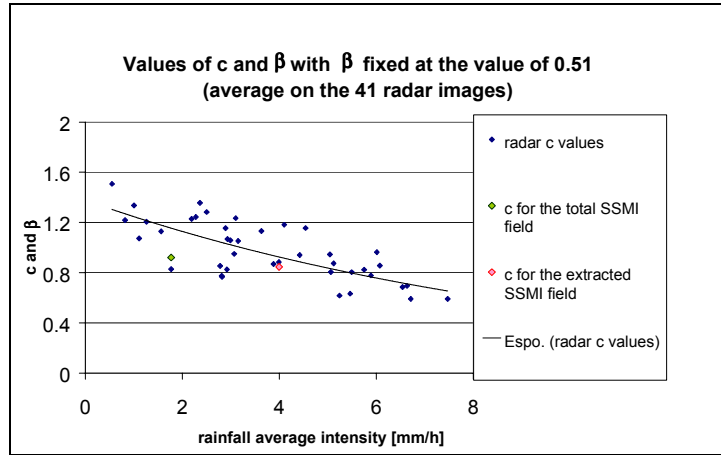


Figure 3.6: log-Poisson coefficients c , keeping $b=0.5$ constant, versus rainfall spatial average intensity for radar values, total SSM/I field and extracted SSM/I field. Continuous line represents the best fit.

3.2 SPACE-TIME ANALYSIS

The space-time analysis requires to make the time variable dimensionally homogeneous to space variables. This homogeneity can be pursued by rescaling the time dimension with a velocity U , so that rainfall can be regarded as a three-dimensional process in the Eulerian coordinate system frozen in time, where two coordinates are for space and the third coordinate is the rescaled time (Ut). This is possible assuming Taylor hypothesis of “frozen turbulence” [Taylor, 1938] to characterize the space-time statistical properties of rainfall as being a three-dimensional homogeneous and isotropic process where a measure on scale 1 along the (rescaled) time axis is the trace of rainfall on a time $\tau=1/U$, but at fixed location.

The advecting velocity U is, in this paper, estimated using a cloud tracking techniques on a sequence of half-hourly Meteosat images in the IR band for the event of October 1998. The entity, which is tracked, is the observed coldest top of the cloud system, not an individual cloud [Bolla et al., 1996]

The average estimated advection velocity of the storm is 13 m/s.

Structure functions (5) of radar images are computed on 7 selected rainfall sequences for scales λ ranging from 8 km to 128 km and time scales ranging from 10 minutes to about 3 hours.

Multifractal exponents $z(q)$ of equation (8) are estimated and presented in Figure 3.7. In the same figure are plotted also the multifractal exponents of rainfall space-time fields for one selected precipitation sequence of GATE 1, characterized by an average rain rate of 2.7 mm/h.

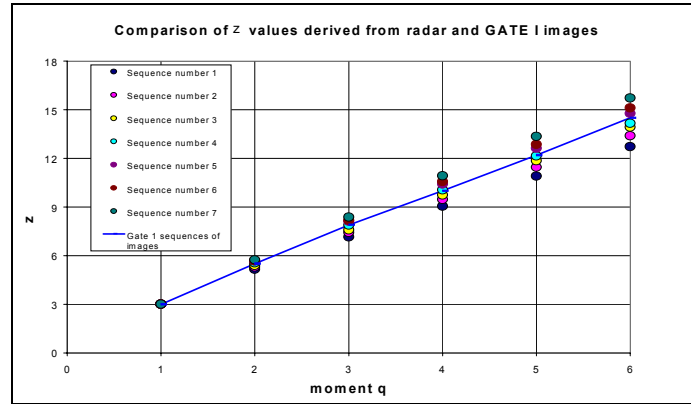


Figure 3.7: values of the exponents $z(q)$ of seven rainfall sequences for spatial scales 1 ranging from 8 km to 128 km and time scales ranging from 10 minutes to 3 hours are compared with the averages of the multifractal exponents estimated from GATE1 datasets.

Sample multifractal exponents (from $q=2$ to 6) are then used to estimate the two log-Poisson parameters c and b of the model by solving the minimization problem (9). Results have shown again a small variability in the estimate of the b parameter for each of the seven sequences of radar rainfall fields. Thus new values for the c parameter are estimated by keeping $b = \text{constant}$ and equal to its mean value 0.5. Results are plotted in Figure 3.8 versus the mean rainfall rate of each sequence. The Figure shows a similar results to that found in the space analysis presented in previous section. Again the dependence of the c parameter on the mean rainfall intensity can be observed.

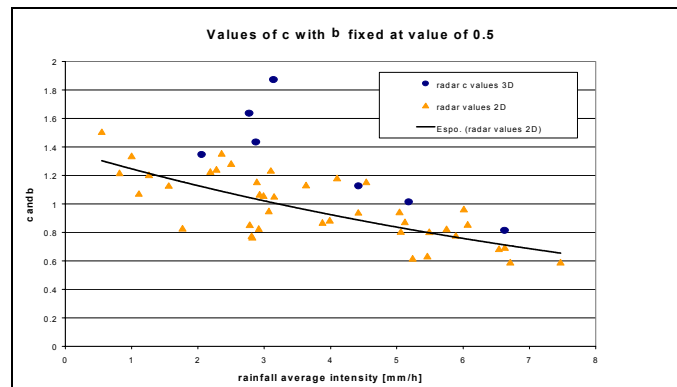


Figure 3.8: log-Poisson coefficients c , keeping $b=0.5$ constant, versus rainfall average intensity for radar datasets in space and for seven rainfall sequences in space-time. Continuous line represents the best fit exponent regression for radar datasets in space.

4 Conclusions

A multifractal analysis of rainfall fields derived from different sensors (the Fossalon radar and the SSM/I) is presented. Results of these analysis have shown that both in space and in space-time domain rainfall fields are characterized by a multifractal structure.

In the space analysis, although the spatial resolution of the radar and SSM/I sensors is different, the slopes of the structure functions are very similar suggesting a possible unique multifractal law for the entire span of scales covered by the two sensors.

As seen from the analysis of the GATE rainfall fields for the 2D and 3D cases there is a dependence of the c parameter from the average field rainfall intensity while the b parameter does not depend from rainfall intensity.

This result states that the large scale rainfall forces the smaller scale statistical properties of precipitation.

In an operational flood forecasting chain it is recommendable to introduce a downscaling tool that is able to share out the large-scale amounts of rainfall predicted by meteorological models down to the smaller catchment's scales.

Acknowledgments

This work has been possible thanks to Dr. S. Dietrich of the Istituto di Fisica dell'Atmosfera, CNR Roma Italy, who kindly made available the SSM/I data. Special thanks go also to Dr. R. Bechini of the Weather Radar Operation Center of ERSR-FVG/CSA, Italy who made available the radar data. This work was supported by the CNR-GNDCI grant 1997-1998 to research unit 3.16.

References

- Bolla, R., Boni, G., La Barbera, P., Lanza, L., Marchese, M. and Zappatore, S. The Tracking and prediction of high intensity rainstorms, *Remote Sensing Reviews*, vol. 14, 151-183, 1996.
- Deidda, R. Multifractal analysis and simulation of rainfall fields in space, *Phys. Chem. Earth (B)*, 24 (1-2), 73-78, 1999.
- Deidda R., Benzi, R., and Siccardi F. Multifractals modeling of anomalous scaling laws in rainfall, *Water Resour. Res.*, 35(6), 1853-1867, 1999.
- Deidda R. Rainfall downscaling in a space-time multifractal framework, *Water Resour. Res.*, submitted, 1999.
- Deidda, R., Ferraris, L., Parodi, U. and Siccardi, F. Remote sensing derived rainfall fields and the estimation of disaggregation parameters, European Geophysical Society XXIV General Assembly, The Hague, 19-23 Aprile, *Geophysical Research Abstracts*, Volume 1, Number 4, 828, 1999.
- Dubrulle, B., Intermittency in fully developed turbulence: log-Poisson statistics and generalized scale-covariance, *Phys. Rev. Lett.*, 73, 959-962, 1994.
- Falconer, K.J., *Fractal geometry: mathematical foundations and applications*, John Wiley and Sons, Inc., Chichester, 1990.
- Feder, J., *Fractals*, Plenum Press, New York, 1988.
- She, Z.-S. and Leveque, E., Universal scaling laws in fully developed turbulence, *Phys. Rev. Lett.*, 72, 336-339, 1994.
- Taylor, G. I., The spectrum of turbulence, *Proc. Roy. Soc. Lon.*, A164(919), 476-490, 1938.